Nonstandard neutrino interactions in a modified ν2HDM

Ujjal Kumar Dey,[1,*] Newton Nath,[2,3,†] and Soumya Sadhukhan[4,‡]

[1]Centre for Theoretical Studies, Indian Institute of Technology Kharagpur, Kharagpur 721302, India
[2]Institute of High Energy Physics, Chinese Academy of Sciences, Beijing 100049, China
[3]School of Physical Sciences, University of Chinese Academy of Sciences, Beijing 100049, China
[4]Physical Research Laboratory, Ahmedabad 380009, India

(Received 10 June 2018; published 5 September 2018)

In the traditional neutrinophilic two-Higgs doublet model (ν2HDM), there is no nonstandard neutrino interaction (NSI) as the interactions between the Standard Model fermions with neutrinos are negligibly small due to the tiny mixing of the two scalar doublets. In this work, we propose that if ν2HDM is modified by considering the right-handed electron, e_R is negatively charged under a global $U(1)$ symmetry; then, one can generate a significant amount of NSI along with the tiny Dirac neutrino mass. Depending on different constraints from the LEP experiment, tree-level lepton flavor violating processes, big-bang nucleosynthesis, etc., we observe that this model significantly restricts the range of permissible NSI parameters, putting a strict upper bound on different NSIs. Furthermore, considering these model-dependent NSIs, we study their impact on the next-generation superbeam experiment, DUNE. We present a detailed discussion on the mass hierarchy sensitivity and the CP-violation discovery study considering the impact of both diagonal and off-diagonal NSIs.

DOI: 10.1103/PhysRevD.98.055004

I. INTRODUCTION

The Standard Model (SM) of particle physics epitomizes our knowledge of fundamental interactions of the subatomic world with all its grandeur. Barring a few minor disagreements, the SM is hitherto untarnished by the direct observations from high energy colliders like the LHC. The most elusive of the particles that constitute the SM is undoubtedly the neutrino, which can very well usher us towards the physics beyond the SM, owing to its perplexing properties: that it is massive (though tiny) and that its different flavors are substantially mixed [1]. These distinct attributes are exotic to the basic tenets of the SM but are experimentally observed. The discovery of neutrino oscillations indubitably established the existence of mass for the neutrinos, whereas in the SM the neutrinos are supposed to be massless. The Super-Kamiokande experiment in Japan published its result to establish the phenomenon of neutrino oscillation in 1998 [2]. Later, various other experiments—such as solar, reactor, and, most recently, long baseline experiments like T2K [3], and NOνA [4]—confirmed the phenomenon of neutrino oscillation. In addition to the confirmation of the presence of neutrino mass, neutrino oscillation results generate some pertinent questions: e.g., (i) the neutrino mass hierarchy, i.e., whether neutrinos obey normal hierarchy (NH, $m_3 > m_2 > m_1$) or inverted hierarchy (IH, $m_3 < m_1 \approx m_2$); (ii) the octant of θ_{23}, i.e., whether θ_{23} lies in the lower octant (LO, $\theta_{23} < 45°$) or in the higher octant (HO, $\theta_{23} > 45°$); and (iii) the determination of the Dirac CP phase δ_{CP}. As the current experiments are striving to resolve the degeneracies in hierarchy and octants and to assess the sensitivity in CP violation (CPV), new theoretical input that can possibly help address these issues is worth exploring. It is thus quite interesting to reconnoiter models that can provide a natural explanation for the tiny neutrino mass along with other issues mentioned above.

The enigma of neutrino mass has led particle physicists to explore various theoretical models that can explain the neutrino mass as well as the observed neutrino mixing angles. Literature on the neutrino mass has been growing for quite some time, and today there are a number of phenomenological models addressing this issue (for a review see [5,6]). Some of the new physics scenarios could lead to corrections to the effective neutrino interactions through higher-dimensional operators. Nonstandard interactions (NSI) of neutrinos can be induced by new physics beyond the SM (BSM). In the BSM scenarios, NSI can arise when the heavier messenger fields are integrated out, which can generate the dimension-6 [7–9] and dimension-8 [10,11]

*ujjal.dey1@gmail.com
†newton@ihep.ac.cn
‡soumyas@prl.res.in

effective operators. For a detailed review and phenomenological consequences, see Refs. [12,13] and the references therein. These were originally discussed even before the establishment of neutrino oscillation phenomena [14–17]. Over the years, many BSM scenarios have been studied where NSIs can be realized. Some of the popular models include the $U(1)$ extended models with a new Z' particle as the messenger, models with single or multiple charged heavy scalars, leptoquark, R-parity violating supersymmetry, etc. [18–24]. Moreover, there are studies which consider the effect of NSI in collider experiments [25–30]. Normally, the extensions of the SM that give rise to NSIs can have stringent constraints from the charged lepton flavor violating (LFV) processes. Therefore, it is imperative to maintain these LFV constraints while building any model from the NSI perspective.

We construct a variant of the neutrinophilic two-Higgs doublet model (ν2HDM) which can have a significant NSI while maintaining various phenomenological constraints. In the standard ν2HDM there is no NSI due to the absence of interaction between left-handed neutrinos and the other leptons and quarks via the extra scalars. We modify the standard ν2HDM such that the second scalar doublet Φ_2 couples only to the electron and neutrinos. This is achieved by assigning a negative charge of the e_R under a global $U(1)$ symmetry. The charged Higgs present in the spectrum couples the left-handed electron and the charged leptons and thus can give rise to NSI by playing the role of the messenger. In this setup we can have different NSI parameters. Apart from the presence of NSI, the hierarchy in the fermion sector is somewhat less drastic in this model compared to the SM. This is because the second Higgs doublet couples only to the electron and neutrinos, and thus it is responsible for the mass of the neutrinos and electron. The first Higgs doublet takes care of all the other SM fermions. Clearly, the hierarchy in the Yukawa couplings is minimized, owing to the two vacuum expectation values (vev) of the two doublets. This betterment in the fermion hierarchy is one of the novel features of this model. Phenomenological constraints characteristic of any 2HDM will also be applicable in this scenario. We consider the constraints on the model parameter space from LFV processes, oblique parameters, μ_{g-2}, big-bang nucleosynthesis (BBN), etc.

Furthermore, we study the impact of model-dependent NSIs in the case of a long baseline (LBL) experiment like DUNE. For DUNE, the mass hierarchy sensitivity considering model-independent bounds on NSI has been studied in [31–34]. These studies show that the mass hierarchy sensitivity of LBL experiments is seriously compromised due to the presence of intrinsic $\epsilon_{ee} \to -\epsilon_{ee} - 2$, $\delta_{CP} \to \pi - \delta_{CP}$ degeneracy. This degeneracy remains true irrespective of baseline and energy. On the other hand, if a LBL experiment like DUNE observes sensitivity, then it will be able to rule out certain parameter space of model-independent NSIs. In the modified ν2HDM model considered here, parameter space of different NSIs is constrained, which helps to avert mass hierarchy degeneracy. We further examine the mass hierarchy sensitivity of DUNE considering model-based NSI parameters. Later, we also address the issue of CPV sensitivity for DUNE. We illustrate the role of the new CP phase on the measurement of δ_{CP} considering both CP-conserving and CP-violating values for the new phases. In our analysis, we assume NSI both in data and in theory. Some of the recent phenomenological studies, considering model-independent bounds of NSI, in the context of DUNE can be found in [31–50] and the references therein.

We organize our paper as follows. In Sec. II, we introduce the concept of nonstandard neutrino interactions and their model-independent bounds. Section III is devoted to a detailed description of the model that has been considered in this work. The traditional ν2HDM model is discussed in the first part, whereas the modification of the model which leads to NSI is discussed in the second part. Various phenomenological constraints coming from LEP data, LFV processes, BBN, etc. are discussed in Sec. IV. We illustrate the effect of diagonal and off-diagonal NSI for DUNE in Sec. V. First, we present our result by considering the appearance channel probability ($P_{\mu e}$). Later, we discuss the impact of NSI on the determination of mass hierarchy sensitivity and the CPV sensitivity in the case of DUNE. Finally, we summarize and conclude our noteworthy findings in Sec. VI.

II. GENERAL DESCRIPTION OF NSI

In this study, we consider the effect of neutral-current NSI in the presence of matter, which is described by the dimension-6 four-fermion operators of the form [14]

$$\mathcal{L}_{\rm NSI}^{NC} = -2\sqrt{2}G_F(\bar{\nu}_\alpha\gamma^\rho P_L\nu_\beta)(\bar{f}\gamma_\rho P_C f)\epsilon_{\alpha\beta}^{fC} + \text{H.c.} \quad (1)$$

where $\epsilon_{\alpha\beta}^{fC}$ are NSI parameters, $\alpha, \beta = e, \mu, \tau$, $C = L, R$, $f = e, u, d$, and G_F is the Fermi constant.[1] Note that, in general, the elements of $\epsilon_{\alpha\beta}$ are complex for $\alpha \neq \beta$ and real for $\alpha = \beta$ due to the Hermitian nature of the interactions. For the matter NSI, $\epsilon_{\alpha\beta}$ are defined as

$$\epsilon_{\alpha\beta} = \sum_{f,C} \epsilon_{\alpha\beta}^{fC} \frac{N_f}{N_e}, \quad (2)$$

where N_f is the number density of fermion f and $\epsilon_{\alpha\beta}^{fC} = \epsilon_{\alpha\beta}^{fL} + \epsilon_{\alpha\beta}^{fR}$. For the Earth's matter, we can assume that the number densities of electrons, protons, and neutrons are equal (i.e., $N_p \simeq N_n = N_e$); in such a case, $N_u \simeq N_d \simeq 3N_e$, and one can write

[1]Note that here we neglect NSI due to charge-current interactions which mainly affect neutrino production and detection [51–56].

$$\epsilon_{\alpha\beta} = \sqrt{\sum_C ((\epsilon^{eC}_{\alpha\beta})^2 + (3\epsilon^{uC}_{\alpha\beta})^2 + (3\epsilon^{dC}_{\alpha\beta})^2)}. \quad (3)$$

The modified Hamiltonian in the presence of propagation NSI, in the flavor basis, can be written as

$$H = \frac{1}{2E}[U\mathrm{diag}(0, \Delta m^2_{21}, \Delta m^2_{31})U^\dagger + \mathrm{diag}(A,0,0) + A\epsilon_{\alpha\beta}], \quad (4)$$

where U is the Pontecorvo-Maki-Nakagawa-Sakata (PMNS) mixing matrix [57], $\Delta m^2_{ij} = m^2_i - m^2_j$ $(i < j = 1, 2, 3)$, $A \equiv 2\sqrt{2}G_F N_e E$ represents the potential arising from standard interactions (SI) of neutrinos in matter, and $\epsilon_{\alpha\beta}$ can be written as

$$\epsilon_{\alpha\beta} = \begin{pmatrix} \epsilon_{ee} & \epsilon_{e\mu} & \epsilon_{e\tau} \\ \epsilon^*_{e\mu} & \epsilon_{\mu\mu} & \epsilon_{\mu\tau} \\ \epsilon^*_{e\tau} & \epsilon^*_{\mu\tau} & \epsilon_{\tau\tau} \end{pmatrix}, \quad (5)$$

where $\epsilon_{\alpha\beta} = |\epsilon_{\alpha\beta}|e^{i\phi_{\alpha\beta}}$ for $\alpha \neq \beta$.

The model-independent bounds [12,58] on these parameters are

$$|\epsilon_{ee}| < 4.2, \quad |\epsilon_{e\mu}| < 0.33, \quad |\epsilon_{e\tau}| < 3.0,$$
$$|\epsilon_{\mu\mu}| < 0.07, \quad |\epsilon_{\mu\tau}| < 0.33, \quad \epsilon_{\tau\tau}| < 21. \quad (6)$$

Having introduced general descriptions of NSI and its model-independent bounds, in the next section we describe our model and calculate the model-dependent bounds of different NSI parameters consistent with different experimental bounds.

III. MODEL DESCRIPTION

For completeness we first discuss the details of the traditional neutrinophilic ν2HDM; for more details see e.g., [59,60] and references therein.[2] In passing we note the reasons for the absence of NSI in the standard scenario. We then modify the vanilla ν2HDM to get the NSI effects.

A. Standard ν2HDM

We start with an extension of the SM by adding an extra scalar doublet Φ_2 having similar gauge quantum numbers as the SM scalar doublet Φ_1. Three right-handed neutrinos (RHN) ν_{Ri} are introduced, and they constitute the Dirac masses with left-handed neutrinos of the SM. There are two main ways to obtain the masses for the neutrinos with this particle spectrum. In one setup [64,65] a $\mathbb{Z}_2$ symmetry is imposed under which the fields Φ_2 and ν_{Ri} are odd and all the SM fields are even. In this setup the Majorana mass terms for ν_{Ri} are not forbidden. In another setup [59], a global $U(1)$ symmetry is imposed, the fields Φ_2 and ν_{Ri} have $+1$ charge, and all the SM fields are neutral. In this scenario the neutrinos exclusively have Dirac masses. For reasons that will be discussed later, we follow the $U(1)$ case closely. In both of these cases the Yukawa interaction of the neutrinos is of the form $(-y^{ij}_\nu \bar{L}_{Li}\tilde{\Phi}_2\nu_{Rj})$, where $L_L = (\nu_L, \ell_L)^T$ is the left-handed lepton doublet and $\tilde{\Phi} = i\sigma_2\Phi^*$. The Yukawa structure of the other SM fermion is of the usual form involving Φ_1. Note that when the $U(1)$ is unbroken, Φ_2 has no vev and the neutrinos remain massless.

The most general scalar potential for the exact $U(1)$ symmetric[3] case is given by

$$V(\Phi_1,\Phi_2) = m^2_{11}\Phi^\dagger_1\Phi_1 + m^2_{22}\Phi^\dagger_2\Phi_2 + \frac{\lambda_1}{2}(\Phi^\dagger_1\Phi_1)^2 + \frac{\lambda_2}{2}(\Phi^\dagger_2\Phi_2)^2 + \lambda_3\Phi^\dagger_1\Phi_1\Phi^\dagger_2\Phi_2 + \lambda_4\Phi^\dagger_1\Phi_2\Phi^\dagger_2\Phi_1. \quad (7)$$

The complex scalar $SU(2)$ doublets Φ_1 and Φ_2 carry hypercharge $Y = +1$. Since in the exact $U(1)$ symmetric case neutrinos are massless, to give masses to neutrinos this symmetry needs to be broken. This is done by introducing a soft-breaking term of the form $(-m^2_{12}\Phi^\dagger_1\Phi_2)$. Clearly, the smallness of m^2_{12} is technically natural in the 't Hooft sense. The two scalar doublets can be presented as

$$\Phi_a = \begin{pmatrix} \phi^+_a \\ (v_a + h_a + i\eta_a)/\sqrt{2} \end{pmatrix}, \quad a = 1,2. \quad (8)$$

The vev of the two scalars can be denoted as $\langle\Phi_1\rangle = v_1$, $\langle\Phi_2\rangle = v_2$, and v_2, responsible for neutrino masses. Therefore, $v_2(\sim\mathrm{eV}) \ll v_1(\sim 246\,\mathrm{GeV})$, while $v^2 = v^2_1 + v^2_2$. In general, the physical scalar fields are given by

$$H^+ = \phi^+_1\sin\beta - \phi^+_2\cos\beta \simeq -\phi^+_2,$$
$$A = \eta_1\sin\beta - \eta_2\cos\beta \simeq -\eta_2, \quad (9a)$$

$$h = -h_1\cos\alpha - h_2\sin\alpha \simeq -h_1,$$
$$H = h_1\sin\alpha - h_2\cos\alpha \simeq -h_2, \quad (9b)$$

where α is the rotation angle for CP-even states and β is for the CP-odd and charged scalar states. These rotations diagonalize the mass matrices with

$$\tan 2\alpha = \frac{2(-m^2_{12} + \lambda_{34}v_1v_2)}{m^2_{12}(v_2/v_1 - v_1/v_2) + \lambda_1 v^2_1 - \lambda_2 v^2_2}, \quad (10)$$

[2] For some other aspects of 2HDM see [61–63].

[3] If instead of the global $U(1)$ one imposes $\mathbb{Z}_2$, then another quartic term of the form $\lambda_5(\Phi^\dagger_1\Phi_2)^2/2$ has to be added to $V(\Phi_1,\Phi_2)$.

$$\tan\beta = \frac{v_2}{v_1}, \tag{11}$$

where $\lambda_{34} \equiv \lambda_3 + \lambda_4$. From the requirement of tiny neutrino mass, we have $v_2 \ll v_1$. Thus, for small m_{12}, both α and β will be very small. From Eqs. (9) it is evident that the SM-like 125-GeV Higgs comes from the doublet Φ_1, whereas the BSM scalars are dominantly comprised of components of the doublet Φ_2. The BSM scalars H, A, $H^\pm$ develop neutrinophilic interactions in the Yukawa sector. The Yukawa couplings of the new scalars in the limit $v_2 \ll v_1$ are described as

$$\mathcal{L}_Y \supset \frac{m_{\nu_i}}{v_2} H\bar{\nu}_i\nu_i - i\frac{m_{\nu_i}}{v_2} A\bar{\nu}_i\gamma_5\nu_i - \frac{\sqrt{2}m_{\nu_i}}{v_2}[U^*_{\ell i}H^+\bar{\nu}_i P_L\ell + \text{H.c.}], \tag{12}$$

where m_{ν_i} are neutrino masses and $U_{\ell i}$ is the PMNS matrix.

In this setup, due to the above-mentioned $U(1)$ charge assignments of the respective fields, left-handed neutrinos cannot couple to right-handed charged leptons through the scalar doublet Φ_1. The possibility of such coupling via the mixing of the other doublet Φ_2 is negligible since that coupling is proportional to $\sin\beta \approx v_2/v_1$, which is negligibly small. Since this type of coupling is needed to generate the NSI effect, in this setup the NSI effect will be negligible.

B. Modified ν2HDM

The standard ν2HDM scenario discussed above cannot give rise to nonstandard interactions in the neutrino sector. Since two different Higgs doublets are responsible for providing mass to the neutrinos and other massive SM particles, there is no interaction of the left-handed neutrinos with the SM massive leptons and quarks. Here we propose to give mass to the electron along with the neutrinos through the second scalar doublet Φ_2. For that purpose, among the SM fields, only the right-handed electron e_R is endowed with the charge (-1) under the global $U(1)$. With this quantum number assignment, the relevant terms for the neutrino and electron sector become

$$\mathcal{L}^m_{\nu 2\text{HDM}} \supset y_e\bar{L}_e\Phi_2 e_R + y_\nu\bar{L}_e\tilde{\Phi}_2\nu_R + \text{H.c.}, \tag{13}$$

where L_e is the SM electron doublet $(\nu_e\ e)^T_L$. Expanding the first term of the Lagrangian gives us terms involving charged Higgs ($H^\pm$) as

$$\mathcal{L}^{\text{Yuk}}_{H^\pm} \supset y_e\bar{\nu}_{eL}H^+e_R + \text{H.c.} \tag{14}$$

This interaction results in the t-channel process of Fig. 1, which can give rise to nonstandard interaction terms between SM neutrinos and electrons. The effective Lagrangian, after integrating out the heavy charged Higgs, is

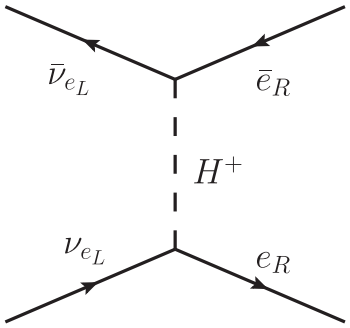

FIG. 1. The Feynman diagram contributing to the NSI in the modified ν2HDM.

$$\mathcal{L}_{\text{eff}} \supset \frac{y_e^2}{4m^2_{H^\pm}}(\bar{\nu}_{eL}\gamma^\rho\nu_{eL})(\bar{e}_R\gamma_\rho e_R) + \text{H.c.} \tag{15}$$

From this effective Lagrangian, comparing it with the defined form of the NSI Lagrangian, Eq. (1), the NSI parameter ϵ_{ee} can be written as

$$\epsilon_{ee} = \frac{1}{2\sqrt{2}G_F}\frac{y_e^2}{4m^2_{H^\pm}}. \tag{16}$$

Note that, in this model, only the right-handed electron contributes in Eq. (3) to provide $\epsilon_{ee} = \epsilon^{eR}_{ee}$. With the same $U(1)$ quantum number assignment, the extra relevant terms for the lepton sector that can be added are

$$\mathcal{L}^m_{\nu 2\text{HDM}} \supset y_1\bar{L}_\mu\Phi_2 e_R + y_2\bar{L}_\tau\Phi_2 e_R + \text{H.c.}, \tag{17}$$

where $L_{\mu/\tau}$ are the SM lepton doublets $(\nu_{\mu/\tau}\ \mu/\tau)^T_L$. These terms provide the following NSI parameters,

$$\epsilon_{e\mu} = \frac{1}{2\sqrt{2}G_F}\frac{y_e y_1}{4m^2_{H^\pm}}, \qquad \epsilon_{e\tau} = \frac{1}{2\sqrt{2}G_F}\frac{y_e y_2}{4m^2_{H^\pm}}, \tag{18a}$$

$$\epsilon_{\mu\tau} = \frac{1}{2\sqrt{2}G_F}\frac{y_1 y_2}{4m^2_{H^\pm}}, \qquad \epsilon_{\mu\mu} = \frac{1}{2\sqrt{2}G_F}\frac{y_1^2}{4m^2_{H^\pm}}. \tag{18b}$$

Note that here the Yukawa couplings y_1, y_2 can be complex. The complex nature of these Yukawa couplings results in generating phases for the NSI parameters.

Before delving into the discussion on phenomenological constraints on this model and the NSI studies, we mention a few of its features. The first term of Eq. (13) appears due to modification in the ν2HDM. The vacuum expectation value of the second doublet v_2 gives mass to the electron here. Thus, using an order-one Yukawa coupling, to get the electron mass $m_e = 0.51$ MeV, we need $v_2 \sim$ MeV. With such a large $v_2 \sim$ MeV, the neutrino Yukawas will be of the order of 10^{-6}. This reintroduces hierarchy in the fermion Yukawa couplings, i.e., the hierarchy of the Yukawas, to accommodate the mass of different fermions ranging from

$\mathcal{O}(\mathrm{eV})$ to $\mathcal{O}(100\ \mathrm{GeV})$, with the same vev. In the SM, if the neutrinos are to be given mass through the SM Higgs mechanism, a hierarchy $\mathcal{O}(10^{12})$ in the Yukawas is required to accommodate the top mass ($y_t \approx 1$) along with the Dirac neutrino ($y_\nu \approx 10^{-12}$) mass, using a vev of 246 GeV. In the general ν2HDM, since the neutrinos are given mass through the second doublet, a hierarchy $\mathcal{O}(10^6)$ is only required to arrange for masses from the top quark to the electron. In our modified ν2HDM, we have a hierarchy $\mathcal{O}(10^6)$ in Yukawa couplings to account for the mass of the electron and neutrinos using the same $v_2 \approx$ MeV. There is another hierarchy $\mathcal{O}(10^3)$ to arrange for the masses of the rest of the fermions, i.e., from the top quark to the muon, using the Φ_1 vev $v_1 \approx 246$ GeV. Distributing the Yukawa hierarchies into two sectors, i.e., $\mathcal{O}(10^6)$ in the $e-\nu$ sector and $\mathcal{O}(10^3)$ in the $t-\mu$ sector, reduces the overall hierarchy of Yukawas in the model in comparison to the SM [where it is $\mathcal{O}(10^{12})$]. However, the modified ν2HDM has two different hierarchies, which is a somewhat less desirable feature than the requirement of only one hierarchy of order 10^6 in the original ν2HDM.

In this modified ν2HDM, leptophilic BSM scalar couplings arise where H (A) couples through the Lagrangian terms

$$\mathcal{L}_{LP} \supset \frac{y_e}{\sqrt{2}} H e_L e_R + i\frac{y_e}{\sqrt{2}} A e_L e_R + \mathrm{H.c.} \tag{19}$$

This coupling has stringent bounds from LEP data, which we discuss in the next section.

Before ending this section, we make a few remarks about the choice of $U(1)$-symmetric ν2HDM over its $\mathbb{Z}_2$ symmetric counterpart. First, in the $\mathbb{Z}_2$ symmetric ν2HDM the CP-even new scalar H is very light, $m_H \sim \mathcal{O}(v_2) \ll v$. For such a light scalar of mass up to the MeV scale, the constraint on the leptophilic coupling is very tight. If ν2HDM with $\mathbb{Z}_2$ is allowed to have an electrophilic scalar coupling, the upper limit on the Yukawa y_e will be of the order of 10^{-4}. This strict bound on y_e mainly comes from the $(g-2)_e$ as can be read off from Fig. 7 of [66]. With a tiny Yukawa coupling which also determines the magnitude of the nonstandard neutrino interaction, NSI effects of the modified model will be negligible. Second, the $\mathbb{Z}_2$ symmetric ν2HDM has been severely constrained from the oblique parameters. The modification of the oblique S parameter due to the presence of a very light neutral scalar m_H pushes it to a large negative value to rule out the model at the 2σ confidence level[4] [60]. In the $U(1)$ case, however, a sufficiently heavy CP-even scalar is possible; in addition, the mass degeneracy of CP-even and CP-odd scalars helps satisfy the T parameter bounds easily.

[4]It has been shown that the introduction of vectorlike leptons relaxes this constraint [67].

IV. PHENOMENOLOGICAL CONSTRAINTS

As is typical in any 2HDM scenario, the parameter space of the present setup will also be subject to constraints from the data pertaining to heavy scalars, flavor violating issues, etc. Note that, in our model, the second doublet couples only to the leptons, and thus the constraints from the LEP and LFV are of more relevance. In this section we discuss constraints on the heavy scalars from the LEP searches, LFV decays, and $(g-2)$, as well as BBN.

A. Constraints from LEP

1. Charged scalar mass

The Z boson decay width measurement at the LEP shows that there is little room for Z decays to BSM particles. This suggests that the new scalars of the modified ν2HDM should be heavier than half of the Z boson mass to kinematically forbid the decays. The search for a charged Higgs at the LEP through the process $e^+e^- \to Z \to H^+H^-$ with $H^\pm$ further decaying to $\tau\nu$ puts a lower bound on the charged Higgs mass as $m_{H^\pm} > 80$ GeV [68].

2. Constraint from $e^+e^- \to l^+l^-$

Measurement of the $e^+e^- \to e^+e^-$ cross section at the LEP experiment can be expressed in terms of a limit on the scale of an effective four-electron interaction as $\lambda > 9.1$ TeV [69]. In modified ν2HDM, the $e^+e^- \to e^+e^-$ process will take place through both the CP-even (H) and CP-odd (A) scalar mediators, and the effective four-lepton operator will be

$$\mathcal{L}_{\mathrm{eff}} \supset \frac{{y_e}^2}{8m_H^2}(\bar{e}_L\gamma^\rho e_L)(\bar{e}_R\gamma_\rho e_R) + \frac{{y_e}^2}{8m_A^2}(\bar{e}_L\gamma^\rho e_L)(\bar{e}_R\gamma_\rho e_R). \tag{20}$$

As in the case of a global $U(1)$-symmetric ν2HDM, the degeneracy of CP-even and CP-odd scalar masses reduces the effective operator as

$$\mathcal{L}_{\mathrm{eff}} \supset \frac{{y_e}^2}{4m_H^2}(\bar{e}_L\gamma^\rho e_L)(\bar{e}_R\gamma_\rho e_R),$$

which, when compared to the effective operator form with a scale Λ, provides the bound on y_e as $y_e^2 \le 8\pi m_H^2/\Lambda^2$. In our modified ν2HDM with global $U(1)$ symmetry, the constraints coming from oblique parameters (S, T) allow mass splitting between the charged scalars and the neutral ones to be largest when $m_{H^\pm}$ is small ($\sim$100 GeV) [60]. For a light charged Higgs the neutral scalar masses can go up to several hundred GeVs. We take $m_H = m_A = 500$ GeV. If higher values of charged Higgs masses are taken, then mass splitting between charged and neutral scalars decreases, which, along with large $m_H^\pm$, constrains the Yukawa coupling

tightly enough to allow very small values of NSI parameters. With $m_H = m_A = 500$ GeV and $\Lambda = 9.1$ TeV the constraint translates to $y_e \leq 0.28$, which further translates to a limit on the vev of Φ_2 as

$$v_2 \geq 2.5 \text{ MeV}. \tag{21}$$

Using this bound we fix the v_2 value at 2.5 MeV to get the tightest limits on other Yukawas y_1, y_2 from LEP measurements in other processes like $e^+e^- \to \mu^+(\tau^+)\mu^-(\tau^-)$.

3. Monophoton constraint

Another LEP constraint arises from the dark matter search in the monophoton signal $e^+e^- \to \text{DM DM}\,\gamma$, where γ is the initial state radiation or it appears due to internal bremsstrahlung. In modified ν2HDM similar monophoton processes can occur, $e^+e^- \to \nu_{e/\tau}\nu_{e/\tau}\gamma$ through the charged Higgs exchange, which couples the right-handed electron with left-handed neutrinos and vice versa. The LEP DM search limit is thus rewritten as

$$y_e^4 + 2y_e^2 y_2^2 + y_2^4 \leq \frac{16 m_{H_\pm}^4}{\Lambda_{\text{DM}}^4}, \tag{22}$$

with DM scale $\Lambda_{\text{DM}} \approx 320$ GeV [70] for light DM particles.[5]

B. Lepton flavor violation constraints

1. $\ell_\alpha \to \ell_\beta \gamma$

For a generic process $\ell_\alpha \to \ell_\beta \gamma$, the scalar mediated branching ratio reads [71]

$$\text{BR}(\ell_\alpha \to \ell_\beta \gamma) = \text{BR}(\ell_\alpha \to e\bar{\nu}\nu)\frac{\alpha_{\text{EM}}}{192\pi}|\langle m_{\alpha\beta}^2\rangle|^2\rho^2. \tag{23}$$

The strongest bound on this type of lepton flavor violating decay comes from the MEG experiment, which gives the upper limit as $\text{BR}(\mu \to e\gamma) < 5.7 \times 10^{-13}$ [72], while bounds on the other LFV decay channels ($\tau \to e\gamma$, $\tau \to \mu\gamma$), obtained from the *BABAR* Collaboration, are weaker. Though lepton flavor violating processes like $\mu \to e\gamma$ happen through the loop driven processes in this model, experimental constraints are strong enough to severely constrain this effect. The branching ratio for this decay, which occurs through the charged scalar mediator, can be written as [73]

$$\text{BR}(\mu \to e\gamma) = \text{BR}(\mu \to e\bar{\nu}\nu)\frac{\alpha_{\text{EM}}}{192\pi}|\langle m_{\mu e}^2\rangle|^2\rho^2, \tag{24}$$

where $\rho = (G_F m_{H^\pm}^2 v_2^2)^{-1}$. In terms of ρ defined here, the 90% confidence level bound reads

$$\rho \lesssim 1.2 \text{ eV}^{-2} \qquad [\mu \to e\gamma]. \tag{25}$$

The limit on ρ translates into a limit where for $v_2 \lesssim 1$ eV one must have $m_H^\pm \gtrsim 250$ GeV. This is the tightest limit so far on the v_2 and $m_{H^\pm}$ parameter space. Limits from similar LFV decay modes are less constraining. The sensitivity of the MEG is expected to be improved further, and the bound on ρ is expected to be improved by about 1 order of magnitude. The limits imposed by the MEG bound on the $(m_{H^\pm}, v_2)$ plane are shown in Fig. 1 of [73].

2. $\tau(\mu) \to 3e$

The LFV decays play a crucial role in constraining the model parameters. From Eq. (17) it is evident that once Φ_2 develops a vev, there is tree-level mixing among the would-be mass eigenstates e, μ, and τ. Therefore, LFV decays like $\tau \to 3e$ and $\mu \to 3e$ are possible in this modified ν2HDM through the neutral scalar (H, A) mediation at tree level and thus imply stringent constraints on the Yukawa couplings y_1 and y_2. Belle results [74] of $\tau \to 3e$ decay can be normalized to $\tau \to \mu\nu_\mu\nu_\tau$ decay as

$$\frac{\Gamma(\tau \to 3e)}{\Gamma(\tau \to \mu\nu_\mu\nu_\tau)} \leq 1.58 \times 10^{-7},$$

which implies that the constraints on ν2HDM parameter space are

$$y_e y_2 \leq \frac{(0.16 m_H)^2}{(1 \text{ TeV})^2}. \tag{26}$$

This is a tighter bound on the $y_e - y_2$ plane compared to the LEP $e^+e^- \to l^+l^-$ and LEP monophoton constraints. Similarly, for $\mu \to 3e$ decay there is an even stronger experimental limit, as $\text{BR}(\mu \to 3e) \leq 1 \times 10^{-12}$ puts a bound on the $y_e - y_1$ plane as

$$y_e y_1 \leq \frac{(8.12 \times 10^{-3} m_H)^2}{(1 \text{ TeV})^2}. \tag{27}$$

For moderate y_e and allowed m_H values, this bound reduces the allowed Yukawa values to a tiny value ($y_1 \sim 10^{-6}$), which makes any NSI parameter involving y_1—like $\epsilon_{e\mu}$, $\epsilon_{\mu\tau}$, $\epsilon_{\mu\mu}$—insignificant. We have not considered this Yukawa coupling in our further analysis. In Fig. 2 we show the $y_2 - v_2$ parameter space allowed by various constraints from the LEP and rare lepton decays. Here the neutral scalar masses m_H, m_A are kept at 500 GeV, where the charged Higgs mass is around 100 GeV. As discussed earlier, the maximal mass difference between neutral and charged scalars is required to enhance NSI

[5] A similar expression for y_1 can also be obtained. However, we see in the next section that a more stringent constraint on y_1 comes from lepton flavor violating decays.

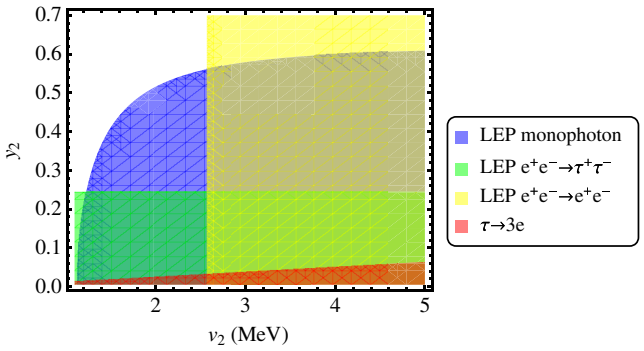

FIG. 2. Allowed region on the $y_2 - v_2$ plane for different LEP constraints. Here m_H, $m_A = 500$ GeV and $m_{H^\pm} \sim 100$ GeV. This is the maximal mass difference allowed from S, T, U, and this maximal mass difference is crucial to generate large NSI values.

parameter values. This is the amount of maximal mass splitting that is allowed from the S, T, U parameters.

C. $g-2$ constraints

The charged scalars can contribute to the muon and electron $g-2$ [75] at one loop, but the contribution is negligible due to a suppression factor $m_l^4/m_{H^\pm}^2$ in the amplitude. Moreover, the loop contribution will depend on the coupling y_1 and since, as we have seen in the last section, $y_1 \sim 10^{-6}$, the contribution will be even more suppressed. Unlike a general 2HDM where the two-loop contributions are dominant, charged lepton couplings to H, A are suppressed here by a factor $\tan\beta$ in ν2HDM, making $g-2$ constraints insignificant in this scenario, as shown in [76].

D. BBN constraints

The new particles that are introduced in this model are the right-handed neutrinos, which are very light, with mass at the eV scale. These new degrees of freedom, ultralight neutrinos can be created in the early Universe to populate it through the process $\bar{l}l \to \nu_R\nu_R$ that occurs through the exchange of the charged scalar $H^\pm$. From BBN there is a limit on new relativistic degrees of freedom, which is $\Delta N_{\rm eff} \equiv N_{\rm eff} - 3.046 = 0.10^{+0.44}_{-0.43}$ at 95% confidence level with He + Planck TT + lowP + BAO data [77]. From this limit one can obtain the decoupling temperature of neutrinos, which for right-handed neutrinos is $T_{d,\nu_R} \approx 200$ MeV and for left-handed ones $T_{d,\nu_L} \approx 3$ MeV [25,78,79]. These considerations put an experimental upper limit on the charged Higgs mediated process $\bar{l}l \to \nu_R\nu_R$ as $(T_{d,\nu_R}/T_{d,\nu_L})^3 \approx (\sigma_L/\sigma_R) = 4(v_2 m_{H^+}/(v_1 m_{\nu_i}|U_{li}|))^4$ [59], which can be translated to a bound on the neutrino Yukawa coupling y_{ν_i} as

$$y_{\nu_i} \leq 0.05 \times \left[\frac{m_{H^\pm}}{100\ \text{GeV}}\right]\left[\frac{1/\sqrt{2}}{|U_{ei}|}\right]. \tag{28}$$

In the usual ν2HDM this constraint is used to put tight constraints on Yukawas. However, in the modified ν2HDM this constraint is trivially satisfied due to the larger values of $v_2 \sim 0.1$ MeV; the preferred y_{ν_i} values are much smaller.

In passing, we also note that this kind of neutrinophilic model can be constrained by the limits on the effective four-neutrino interactions [80–82]. In ν2HDM the effective 4ν interactions can occur through the neutral CP-even and CP-odd BSM scalar propagators. For a ν2HDM with a global $U(1)$ symmetry, the BSM neutral scalars will be heavier, with masses around 100 GeV, which suppresses the effective interaction rate. Therefore, even with $H(A)\nu\nu$ Yukawa couplings $\sim$1, the effective four-neutrino vertex strength remains sufficiently low to stay below the experimental limits on the effective four-neutrino interaction.

V. STUDY OF NSI

In this section, we first present a discussion on the constraint range of NSI parameters in this model. Furthermore, we proceed with a detailed study of these bounds, considering the data from DUNE. Our initial discussion is on the impact of model-dependent NSI, considering the appearance channel probability for both neutrinos and antineutrinos. Moreover, we also perform a substantially detailed study at the χ^2 level where we illustrate the impact of NSI on mass hierarchy sensitivity and the CP-violation discovery study.

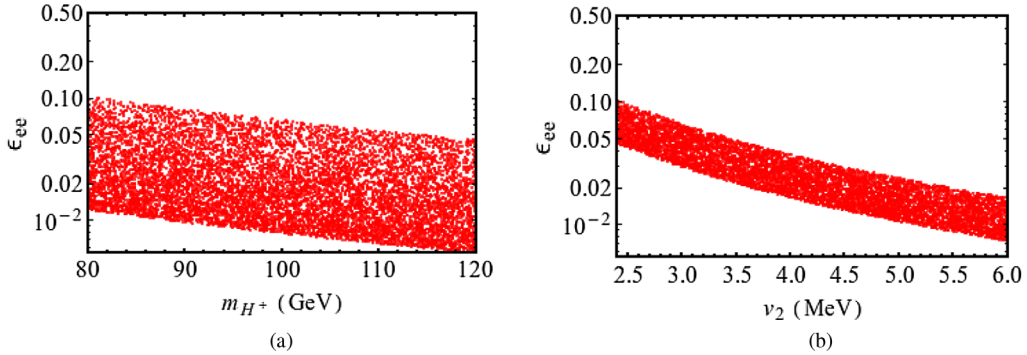

FIG. 3. Allowed values of NSI parameter ϵ_{ee} for a random scan of parameters and its distribution with (a) charged Higgs mass $m_{H^\pm}$ and (b) the vacuum expectation value of Φ_2, v_2 (right).

TABLE I. *Benchmark points and* ϵ_{ee}. NSI parameter ϵ_{ee} for different benchmark values of v_2, where the charged Higgs mass is varied over a range from 80 GeV to 100 GeV (keeping in mind mass splitting allowed by oblique parameter considerations and mass splitting required for satisfying LEP limits) for each v_2 value.

Parameters	Benchmark point I	Benchmark point II	Benchmark point III
v_2	2.5 MeV	3 MeV	5 MeV
$m_{H^\pm}$	80–100 GeV	80–100 GeV	80–100 GeV
ϵ_{ee}	0.061–0.095	0.042–0.066	0.015–0.024

A. NSI in the modified ν2HDM

Here we fix different benchmark values of v_2 and vary $m_{H^\pm}$ in the range of 80–120 GeV. The LEP bound sets the lower limit of the charged Higgs mass at 80 GeV. To satisfy the LEP $e^+e^- \to l^+l^-$ constraint, we need to have heavier electrically neutral BSM scalars that can keep the cross section low. On the other hand, the heavier charged Higgs will suppress the values of nonstandard neutrino interaction parameters, as can be seen from Eq. (16). Therefore, it is optimal to have a maximal splitting between charged and neutral BSM scalars, and the splitting is controlled by oblique parameter constraints. Maximal splitting is possible for a smaller mass of the charged scalar up to $m_H^\pm = 120$ GeV when the neutral scalar masses are at 500 GeV. So, the upper limit of $m_{H^\pm}$ is chosen at 120 GeV. From the LEP upper limit on the $e^+e^- \to e^+e^-$ process, a lower bound on the v_2 value can be obtained as $v_2 \leq 2.5$ MeV. For three different values of $v_2 \geq 2.5$ MeV, we choose three benchmark points and calculate ϵ_{ee} for those values. The allowed values of ϵ_{ee} for various model parameters m_{H^+} and v_2 are shown in Fig. 3. From this, we take some representative benchmark points for ϵ_{ee} along with v_2 and m_{H^+} which are given in Table I.

Constraints from lepton flavor violating decay $\mu \to 3e$ force the Yukawa coupling y_1 to be small, i.e., of the order of 10^{-6}, so that all the ϵ values involving μ, i.e., $\epsilon_{e\mu}, \epsilon_{\mu\mu}, \epsilon_{\mu\tau}$, will be negligible and not have any significant effect on the observables. Thus, we do not consider those NSI parameters for our analysis. The only NSI parameters that we explore are $\epsilon_{e\tau}$ and $\epsilon_{\tau\tau}$. In general, the model-independent constraint on the NSI parameter $\epsilon_{\tau\tau}$ is too loose to put any significant constraint on the model parameters. For the case of y_2, the tightest bound comes from LFV decay $\tau \to 3e$, which restricts y_2 to be below 0.035 for $v_2 = 2.5$ MeV, and this upper limit increases with v_2. We have chosen different values of Yukawa coupling y_2 within this limit. For these different y_2 values, $\epsilon_{e\tau}$ numbers at three benchmark points are given in Table II.

TABLE II. NSI parameter $\epsilon_{e\tau}$ for three benchmark points (BP I, II, III) for different values of y_2.

BP I ($v_2 = 2.5$ MeV)			
y_2	0.01	0.02	0.035
$\epsilon_{e\tau}$	0.0021–0.0033	0.0043–0.0067	0.0075–0.0117
BP II ($v_2 = 3.0$ MeV)			
y_2	0.01	0.02	0.04
$\epsilon_{e\tau}$	0.0018–0.0028	0.0036–0.0056	0.0071–0.011
BP III ($v_2 = 5.0$ MeV)			
y_2	0.02	0.04	0.065
$\epsilon_{e\tau}$	0.0021–0.0033	0.0043–0.0067	0.007–0.011

B. Probability level descriptions

We now study the appearance channel ($P_{\mu e}$) probability in the case of DUNE, considering model-dependent NSI parameters ϵ_{ee} and $\epsilon_{e\tau}$. The relevant analytical expression for the appearance channel probability in the case of normal hierarchy (NH), considering s_{13}, $r = \Delta m^2_{21}/\Delta m^2_{31}$ and $\epsilon_{\alpha\beta}$ as small parameters, except $\alpha, \beta = e$, can be written as [31]

$$\begin{aligned} P_{\mu e} &= x^2 f^2 + 2xyfg\cos(\Delta + \delta_{CP}) + y^2 g^2 \\ &\quad + 4\hat{A}\epsilon_{e\tau} s_{23} c_{23}\{xf[f\cos(\phi_{e\tau} + \delta) - g\cos(\Delta + \delta + \phi_{e\tau})] \\ &\quad - yg[g\cos\phi_{e\tau} - f\cos(\Delta - \phi_{e\tau})]\} \\ &\quad + 4\hat{A}^2(g^2 + f^2)c^2_{23}s^2_{23}|\epsilon_{e\tau}|^2 - 8\hat{A}^2 fgs_{23}c_{23}c_{23}\epsilon^2_{e\tau}\cos\Delta \\ &\quad + \mathcal{O}(s^2_{13}\epsilon, s_{13}\epsilon^2, \epsilon^3), \end{aligned} \tag{29}$$

where

$$\begin{aligned} & x = 2s_{13}s_{23}, \qquad y = 2rs_{12}c_{12}c_{23}, \\ & (s_{ij} = \sin\theta_{ij}, c_{ij} = \cos\theta_{ij}, ij = 12, 13, 23), \\ & \Delta = \frac{\Delta m^2_{31} L}{4E}, \qquad \hat{A} = \frac{A}{\Delta m^2_{31}}, \\ & f, \bar{f} = \frac{\sin[\Delta(1 \mp \hat{A}(1 + \epsilon_{ee}))]}{(1 \mp \hat{A}(1 + \epsilon_{ee}))}, \\ & g = \frac{\sin[\hat{A}(1 + \epsilon_{ee})\Delta]}{\hat{A}(1 + \epsilon_{ee})}. \end{aligned} \tag{30}$$

A similar expression for the inverted hierarchy (IH) can be calculated by replacing $\Delta m^2_{31} \to -\Delta m^2_{31}$ [i.e., $\Rightarrow \Delta \to -\Delta$, $\hat{A} \to -\hat{A}$ (i.e., $f \to -\bar{f}$ and $g \to -g$), $y \to -y$]. Also, the expressions for antineutrino probability ($P_{\bar{\mu}\bar{e}}$) can be obtained by replacing $\hat{A} \to -\hat{A}$ ($\Rightarrow f \to \bar{f}$), $\delta_{CP} \to -\delta_{CP}$.

DUNE has been proposed as a next generation superbeam experiment at Fermilab, USA [83–87]. It will use the existing Neutrinos at the Main Injector (NuMI) beamline design at Fermilab as a source of neutrinos. Its far detector will be placed at the Sanford Underground Research Facility (SURF) in Lead, South Dakota, at a distance of 1300 km from the source. DUNE Collaboration plans to

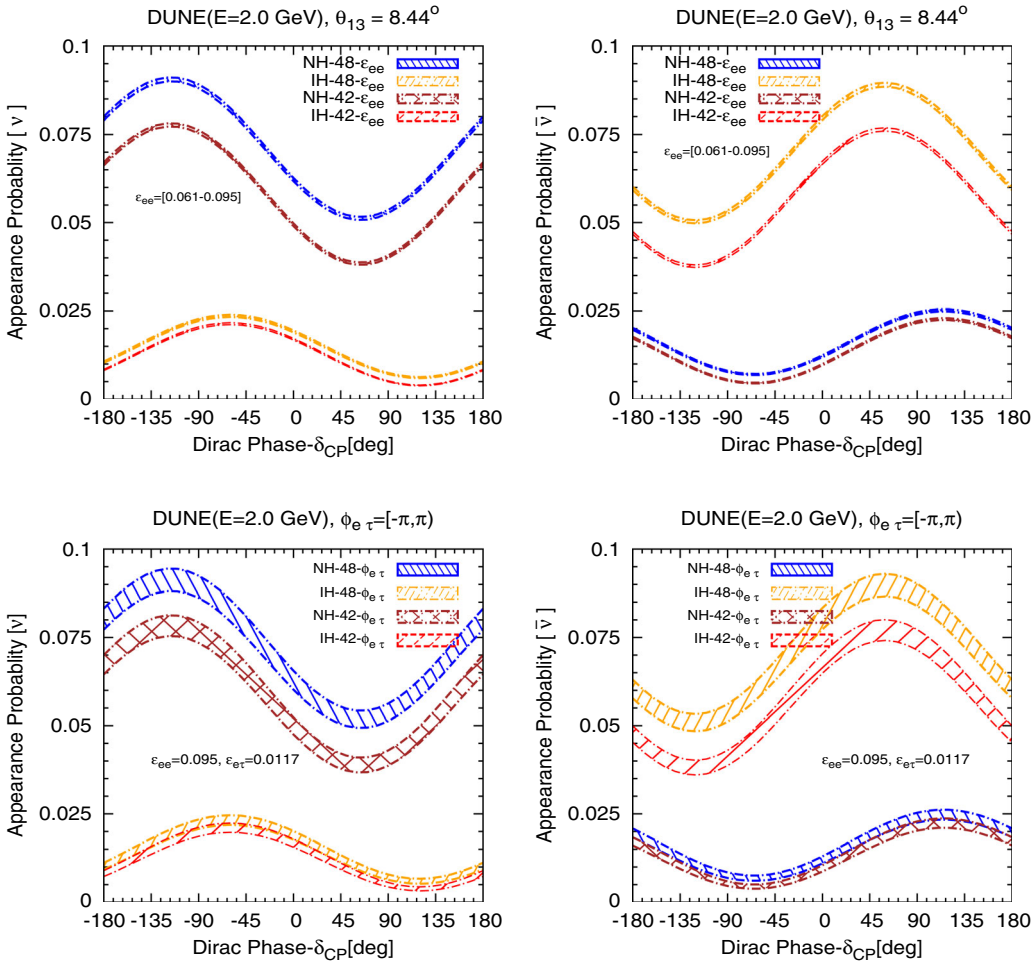

FIG. 4. Appearance channel probability vs δ_{CP} for DUNE, considering neutrinos (antineutrinos) in the left (right) panel. Here the top (bottom) row represents the oscillation probability in the presence of the diagonal (off-diagonal) NSI parameter ϵ_{ee} ($\epsilon_{e\tau}$).

use a liquid argon time-projection chamber (LArTPC) detector with a volume of 10 kton and 40 kton corresponding to the first phase and final phase, respectively. In our simulation, we consider the 10 kton detector volume. We also consider the flux corresponding to 1.2 MW beam power with 120 GeV protons that give 1×10^{21} protons on target (POT) per year. In the analysis, we use the method of pulls [88,89] as outlined in [90] to account for systematic errors. For the numerical simulation, we use the GLoBES package [91,92] along with the required auxiliary files [93,94]. The remaining details of the DUNE and numerical specifications considered here are the same as in [95]. We have also added a 5% prior on $\sin^2 2\theta_{13}$.

In Fig. 4, we discuss the appearance channel probability ($P_{\mu e}$) considering the diagonal NSI parameter ϵ_{ee} in the top row, whereas in the bottom row, we show our results considering the off-diagonal NSI parameter $\epsilon_{e\tau}$ with 2 GeV neutrino beam energy. We present our results considering neutrinos (antineutrinos) in the left (right) panel. Depending on the true hierarchy and true octant, we have four combinations of hierarchy-octant, namely, NH-HO, NH-LO, IH-HO, and IH-LO. We discuss our results for all four possibilities. The tiny bands in the top row are over the range of the model-dependent NSI parameter ϵ_{ee} as given by the first column of Table I.[6] In the bottom row, we describe the role of the off-diagonal NSI parameter, where different bands are over the range of the new CP phase $\phi_{e\tau}$ (see figure legends for details). Note that in the bottom row, to have a better understanding of the new CP phase, we fix the value of the NSI parameters, and the representative value of $\epsilon_{e\tau}$ is taken from Table II. A general probability-level discussion, considering a similar setup, in the absence of NSI on various degenerate solutions is given in Ref. [95], whereas some noteworthy issues considering model-independent NSI parameters are presented in Ref. [33] considering DUNE.

We concentrate here on the impact of model-dependent NSI parameters. In the literature (see [31–34]), it was pointed out that the appearance channel probability suffers from

[6]Note that, for illustrative purposes, we describe our results considering one set of solutions.

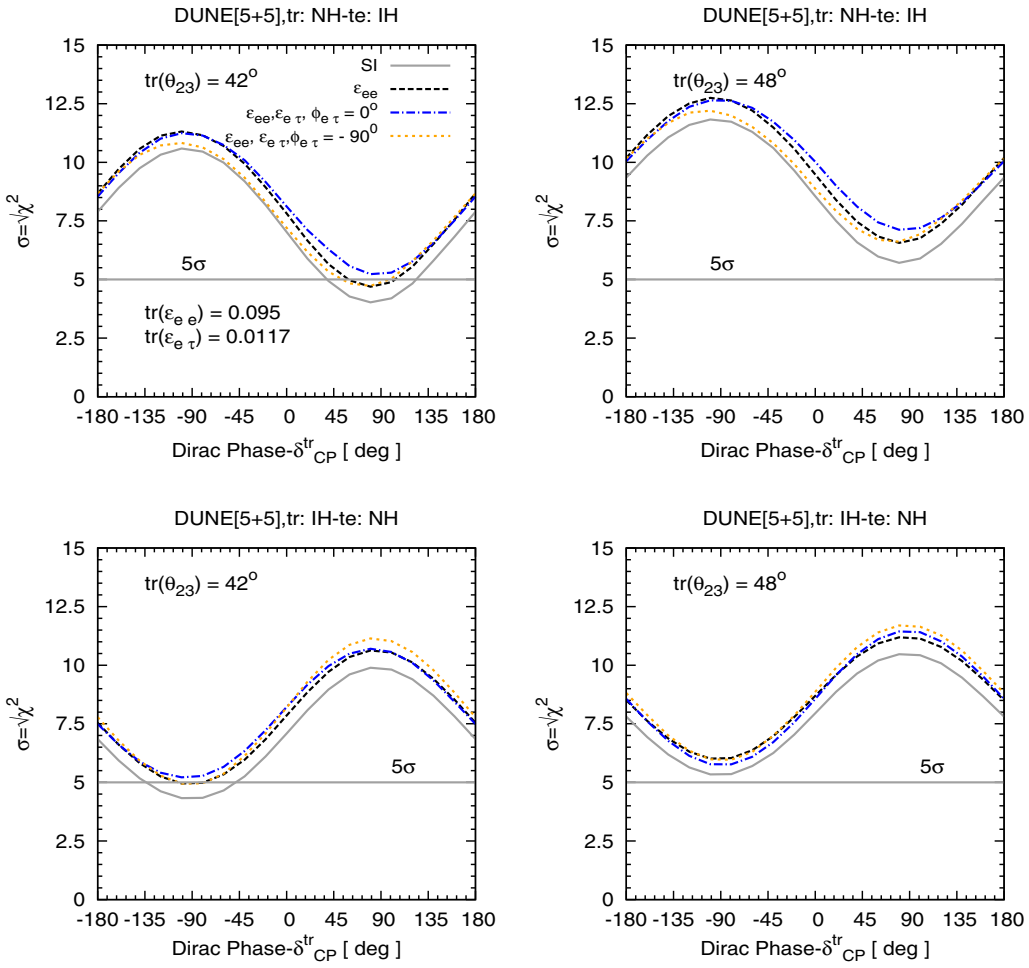

FIG. 5. Hierarchy χ^2 for DUNE in the presence of NSI. Here the top (bottom) row is for true NH (IH) and the left (right) column is for LO (HO).

degeneracy due to the transformation of the form $(\mathrm{NH}, \epsilon_{ee}) \to (\mathrm{IH}, -\epsilon_{ee} - 2)$ and $(\mathrm{NH}, \delta_{CP}) \to (\mathrm{IH}, \pi - \delta_{CP})$ in the presence of model-independent NSI parameters. Here we notice, considering our model-dependent constrained parameter space of ϵ_{ee}, that DUNE has no hierarchy degeneracy, as shown in the first plot of the top row in Fig. 4. This can be understood by comparing NH bands (blue, brown) with IH bands (yellow, red), as the former have no intersection with the latter. The underlying reason for the absence of this degeneracy can be traced back to the fact that the transformation required for this degeneracy, $(\mathrm{NH}, \epsilon_{ee}) \to (\mathrm{IH}, -\epsilon_{ee} - 2)$, cannot be realized in our model, as ϵ_{ee} is always positive, as can be seen from Eq. (16). In the first plot of the bottom row, we also observe that $P_{\mu e}$ has no hierarchy degeneracy even in the presence of the off-diagonal NSI parameter $\epsilon_{e\tau}$. Note that with the inclusion of $\epsilon_{e\tau}$, the width of different bands become broader; this is due to the unconstrained range of the new CP phase $\phi_{e\tau}$, which affects the measurement of the Dirac CP phase. Similar results are also observed for antineutrinos, as shown by the right panel, and the conclusion made for neutrinos remains the same for antineutrinos. Moreover, to understand the impact of NSI on the determination of hierarchy and CP-violation sensitivity, we extend the study using our model-dependent NSI parameters at the χ^2 level. In the next section, we illustrate the details.

C. Sensitivity study

We now discuss the mass hierarchy sensitivity as well as the CP-violation sensitivity of DUNE with model-dependent NSI parameters. For comparison, we also describe our results considering SI. Throughout the study, we consider [5+5] years run time for DUNE.[7] In Fig. 5, we describe our results for the mass hierarchy sensitivity considering true θ_{23} as 42° for lower octant (LO) and 48° for higher octant (HO) in the first and second panels, respectively. In the top (bottom) row, we present our results considering true hierarchy as NH (IH), marginalized over test hierarchy. We take true values of other neutrino parameters as $\sin^2\theta_{12} = 0.321$, $\sin^2 2\theta_{13} = 0.085$, $\Delta m^2_{31} = 2.50 \times 10^{-3}$ eV^2, and $\Delta m^2_{21} = 7.56 \times 10^{-5}$ eV^2,

[7]Note that $[5 + 5]$ means we divide the total exposure by 5 years of neutrino run and another 5 years of antineutrino run.

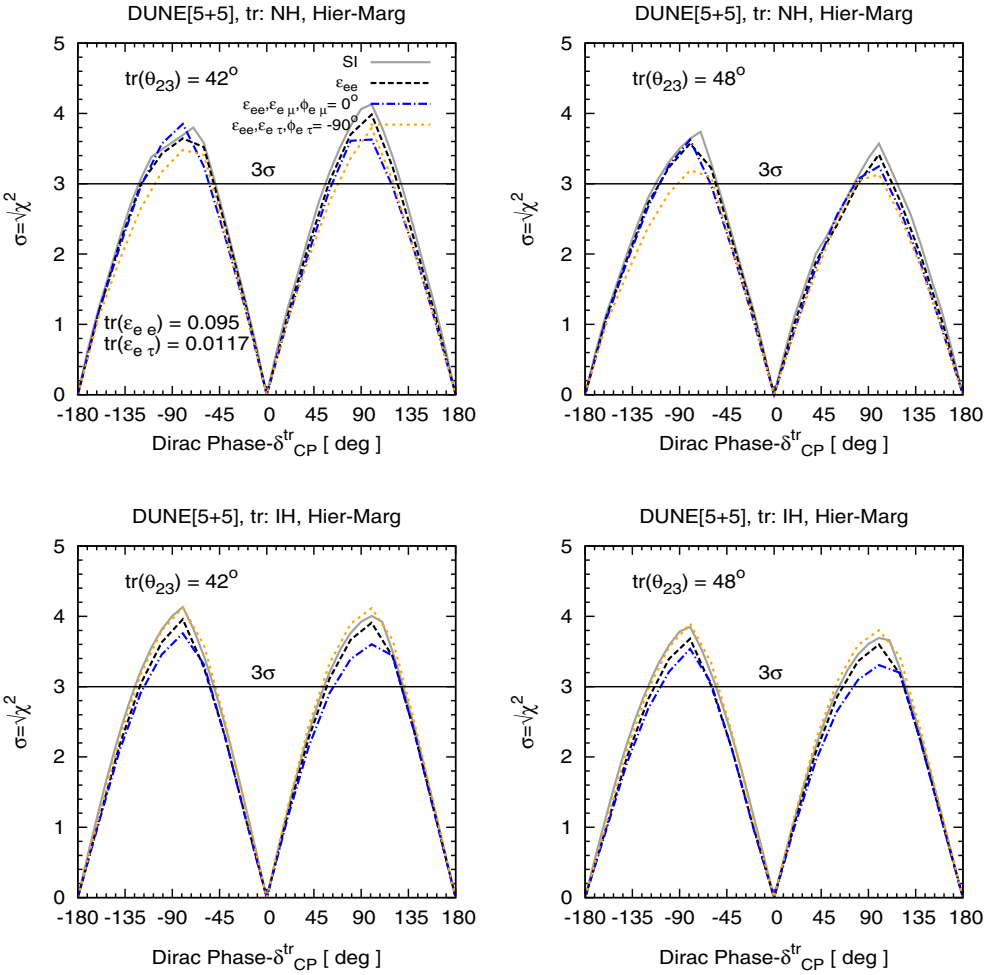

FIG. 6. *CP*-violation discovery χ^2 for DUNE in the presence of NSI. Here the top (bottom) row is for NH (IH), whereas in the left (right) panel, we show results for LO (HO).

which are compatible with the current global-fit data [96–98]. In test hierarchy, we marginalize over their 3σ ranges.[8] For the NSI parameters, we marginalize over test ϵ_{ee} considering the range as given in BP I of Table I, whereas we keep a fixed value for the off-diagonal NSI parameter as given in Table II (see figure legends for details). This benchmark point is chosen since the respective v_2 value satisfies all other constraints and is well within the allowed parameter region. Note that the four different curves correspond to SI (gray solid), the diagonal NSI parameter ϵ_{ee} (black long-dotted), the off-diagonal NSI parameter $\epsilon_{e\tau}$ with $\phi_{e\tau} = 0°$ (blue dash-dotted), and $\phi_{e\tau} = -90°$ (yellow dotted), respectively. We quantify our mass hierarchy sensitivity as

$$\chi^2_{\mathrm{NH-IH}} = \min \sum_i \frac{[N_i(\mathrm{NH}^{\mathrm{tr}}, \epsilon^{\mathrm{tr}}, \phi^{\mathrm{tr}}) - N_i(\mathrm{IH}^{\mathrm{te}}, \epsilon^{\mathrm{te}}, \phi^{\mathrm{tr}})]^2}{\sigma[N_i(\mathrm{NH}^{\mathrm{tr}}, \epsilon^{\mathrm{tr}}, \phi^{\mathrm{tr}})]^2}, \tag{31}$$

where N_i represents the number of events for the ith oscillation parameters. Also, $\epsilon \equiv \epsilon_{\alpha\beta}$ are marginalized for $\alpha = \beta = e$ and kept fixed in both true and test for $\alpha \neq \beta$, whereas $\phi \equiv \phi_{\alpha\beta}$ are considered fixed in both true and test to calculate N. We discuss our results considering a benchmark of 5σ C.L. as shown by the horizontal line.

From the gray curve, we observe that DUNE can reach 5σ hierarchy sensitivity with the 10 kton detector mass, independent of the true values of δ_{CP} and irrespective of the nature of true hierarchy NH or IH, in the case of HO (right panel) for SI. For LO (left panel), we notice it achieves 5σ hierarchy sensitivity for all the true values of δ_{CP} except the regions around true $\delta_{CP} = +90°$ for neutrinos. In the presence of ϵ_{ee} (see black long-dotted curve), we find that DUNE achieves greater than or almost equivalent to 5σ sensitivity for all the mentioned cases. Considering $\epsilon_{e\tau}$, we describe our results for both *CP*-conserving (i.e., when $\phi_{e\tau} = 0°$) as well as *CP*-violating (i.e., when $\phi_{e\tau} = -90°$) values of the new *CP* phase. In the case of HO, we notice that even in the presence of off-diagonal NSI parameters, DUNE can achieve 5σ hierarchy sensitivity for all the true

[8]Note that we do not marginalize over θ_{12}.

values of δ_{CP}. In the case of LO, we find that DUNE attains 5σ hierarchy sensitivity irrespective of the true values of δ_{CP} for all the cases except the regions around true $\delta_{CP} = +90°$. Similar results hold for the case of true IH as shown by the bottom row, except that for IH, the minimum is near true $\delta_{CP} = -90°$.

In Fig. 6, we discuss *CPV* discovery χ^2 for DUNE considering both SI and NSI. The left (right) panel describes our results for LO (HO), whereas the top (bottom) row shows our results for true hierarchy as NH (IH). The true values that we consider correspond to $\epsilon_{ee} = 0.095$, $\epsilon_{e\tau} = 0.0117$ and are based on our model as given in Tables I and II; for the new *CP* phase due to NSI, we take two cases, namely, *CP*-conserving (0°) and *CP*-violating (−90°) values. We describe *CPV* discovery χ^2 as

$$\chi^2_{CPV} = \min \sum_i \frac{[N_i(\delta^{\rm tr}_{CP}, \epsilon^{\rm tr}, \phi^{\rm tr}) - N_i(\delta^{\rm te}_{CP}(0°, \pm 180°), \epsilon^{\rm te}, \phi^{\rm tr})]^2}{\sigma[N_i(\delta^{\rm tr}_{CP}, \epsilon^{\rm tr}, \phi^{\rm tr})]^2}, \tag{32}$$

where N_i represents the number of events for the ith oscillation parameters. Also, ϵ, ϕ are defined as in Eq. (31). We draw a 3σ line as a benchmark for the discussion of our results. Comparing all curves, we notice that DUNE achieves maximum *CPV* discovery sensitivity for the SI compared to NSI parameters. However, considering the diagonal NSI parameter, we find that it gives almost equal *CP* sensitivity as SI at 3σ C.L. for both hierarchies. Further, when we add off-diagonal NSI parameters to the diagonal NSI parameter, as shown by the blue dot-dashed and yellow dotted curves, we observe that *CPV* sensitivity reasonably decreases for NH. However, for IH we find that *CPV* sensitivity is enhanced for *CP*-violating values compared to *CP*-conserving values. Thus, an extra *CP* phase complicates the measurement of the Dirac-*CP* phase (δ_{CP}) and hence affects the measurement of overall *CP* sensitivity even in the case of the constraint parameter space of NSIs.

VI. SUMMARY AND CONCLUSION

Neutrino oscillation experiments opened a new vista to probe the fundamental properties of neutrinos. New physics models, incorporating neutrino masses, are testable in these experiments via the oscillation data. Many of these BSM scenarios give rise to NSI that can be tested in the oscillation experiments. But such models are constrained because of lepton flavor violation issues.

The traditional ν2HDM is one of the popular models that tries to explain neutrino masses by extending the SM with two scalar doublets and right-handed neutrinos. However, this model produces a negligible amount of NSI due to the almost nonexistent interaction of the SM charged leptons and quarks with the neutrinos, determined by the tiny mixing ($\approx v_1/v_2$) of the two scalar doublets. In this study, we propose a modified ν2HDM, which is an improvement over the usual ν2HDM. We can have a sizable NSI parameter while maintaining LFV constraints. We achieve this by assigning a charge to e_R under a global $U(1)$ symmetry. This can lead to an observationally significant NSI, along with the presence of a tiny Dirac neutrino mass, keeping the original motivation of ν2HDM intact. This modification of ν2HDM reintroduces hierarchy in the Yukawas in the $e-\nu$ sector but simultaneously eases the hierarchy in the $t-\mu$ side, compared to that in the traditional ν2HDM. Softly broken global $U(1)$ ν2HDM allows the presence of a heavy neutral BSM scalar, which helps us to address the stringent bound on the electrophilic Yukawa of an ultralight neutral scalar as well as the tight constraints from the oblique parameter (S, T, U) measurements. Combined effects of the LEP constraints like the $e^+e^- \to l^+l^-$, monophoton search, along with the bound on $H^\pm$ mass, reduce a significant amount of allowed parameter space of the modified ν2HDM case, therefore putting stringent bounds on the NSI parameters. The presence of LFV decays like $\tau \to 3e$, $\mu \to 3e$ puts a stringent upper bound on the Yukawa couplings y_1, y_2, and that results in any NSI parameter involving y_1 being negligible apart from a significant reduction of the upper bound of other NSI parameters.

Depending on these constraints, this model predicts the range of permissible NSI parameter ϵ_{ee}. We also find that the only possible off-diagonal NSI parameter in this model is $\epsilon_{e\tau}$, whereas remaining NSIs become insignificant under model constraints. Thus, the effects of NSI parameters involving y_1, such as $\epsilon_{e\mu}$, $\epsilon_{\mu\mu}$, etc., are not studied here. Later, we study the impact of these NSIs considering LBL experiments like DUNE. At the probability level, considering model-dependent NSIs, we do not observe any wrong hierarchy degeneracy, even in the presence of off-diagonal NSI parameters. Furthermore, at the χ^2 level, we find that DUNE shows around 5σ hierarchy sensitivity when one adopts NH as well as IH as a true hierarchy, considering one at a time. These results remain valid irrespective of the value of the true Dirac *CP* phase, δ_{CP}. From our study of *CP* discovery, we notice that *CP* violation in the leptonic sector is affected even in the presence of model-dependent diagonal NSI parameters. Further, we observe that an extra *CP* phase, due to off-diagonal NSI parameters, complicates the measurement of the Dirac-*CP* phase and hence affects the measurement of overall *CP* sensitivity.

ACKNOWLEDGMENTS

U. K. D. acknowledges support from the Department of Science and Technology, Government of India under the fellowship reference number PDF/2016/001087 (SERB National Post-Doctoral Fellowship). U. K. D. thanks Dr. Tirtha Sankar Ray for useful discussions. The research work of N. N. was supported in part by the National Natural Science Foundation of China under Grant No. 11775231. The authors would like to thank Professor Srubabati Goswami for her insightful comments and a careful reading of the manuscript.

[1] T. Ohlsson, Special issue on "Neutrino oscillations: Celebrating the nobel prize in physics 2015," Nucl. Phys. **B908**, 1 (2016).
[2] Y. Fukuda *et al.* (Super-Kamiokande Collaboration), Evidence for Oscillation of Atmospheric Neutrinos, Phys. Rev. Lett. **81**, 1562 (1998).
[3] K. Abe *et al.* (T2K Collaboration), Combined Analysis of Neutrino and Antineutrino Oscillations at T2K, Phys. Rev. Lett. **118**, 151801 (2017).
[4] P. Adamson *et al.* (NOνA Collaboration), Constraints on Oscillation Parameters from ν_e Appearance and ν_μ Disappearance in NOνA, Phys. Rev. Lett. **118**, 231801 (2017).
[5] S. F. King, Models of neutrino mass, mixing and CP violation, J. Phys. G **42**, 123001 (2015).
[6] Y. Cai, J. Herrero-García, M. A. Schmidt, A. Vicente, and R. R. Volkas, From the trees to the forest: A review of radiative neutrino mass models, Front. Phys. **5**, 63 (2017).
[7] W. Buchmuller and D. Wyler, Effective Lagrangian analysis of new interactions and flavor conservation, Nucl. Phys. **B268**, 621 (1986).
[8] S. Bergmann and Y. Grossman, Can lepton flavor violating interactions explain the LSND results?, Phys. Rev. D **59**, 093005 (1999).
[9] S. Bergmann, Y. Grossman, and D. M. Pierce, Can lepton flavor violating interactions explain the atmospheric neutrino problem?, Phys. Rev. D **61**, 053005 (2000).
[10] Z. Berezhiani and A. Rossi, Limits on the nonstandard interactions of neutrinos from e^+e^- colliders, Phys. Lett. B **535**, 207 (2002).
[11] S. Davidson, C. Pena-Garay, N. Rius, and A. Santamaria, Present and future bounds on nonstandard neutrino interactions, J. High Energy Phys. 03 (2003) 011.
[12] T. Ohlsson, Status of non-standard neutrino interactions, Rep. Prog. Phys. **76**, 044201 (2013).
[13] O. G. Miranda and H. Nunokawa, Non standard neutrino interactions: Current status and future prospects, New J. Phys. **17**, 095002 (2015).
[14] L. Wolfenstein, Neutrino oscillations in matter, Phys. Rev. D **17**, 2369 (1978).
[15] J. W. F. Valle, Resonant oscillations of massless neutrinos in matter, Phys. Lett. B **199**, 432 (1987).
[16] E. Roulet, MSW effect with flavor changing neutrino interactions, Phys. Rev. D **44**, R935 (1991).
[17] M. M. Guzzo, A. Masiero, and S. T. Petcov, On the MSW effect with massless neutrinos and no mixing in the vacuum, Phys. Lett. B **260**, 154 (1991).
[18] Y. Farzan and M. Tortola, Neutrino oscillations and nonstandard interactions, Front. Phys. **6**, 10 (2018).
[19] M. S. Bilenky and A. Santamaria, One loop effective Lagrangian for a standard model with a heavy charged scalar singlet, Nucl. Phys. **B420**, 47 (1994).
[20] J. Barranco, O. G. Miranda, and T. I. Rashba, Low energy neutrino experiments sensitivity to physics beyond the Standard Model, Phys. Rev. D **76**, 073008 (2007).
[21] S. Antusch, J. P. Baumann, and E. Fernandez-Martinez, Non-standard neutrino interactions with matter from physics beyond the Standard Model, Nucl. Phys. **B810**, 369 (2009).
[22] M. Malinsky, T. Ohlsson, and H. Zhang, Non-standard neutrino interactions from a triplet seesaw model, Phys. Rev. D **79**, 011301 (2009).
[23] T. Ohlsson, T. Schwetz, and H. Zhang, Non-standard neutrino interactions in the Zee-Babu model, Phys. Lett. B **681**, 269 (2009).
[24] D. V. Forero and W.-C. Huang, Sizable NSI from the $SU(2)_L$ scalar doublet-singlet mixing and the implications in DUNE, J. High Energy Phys. 03 (2017) 018.
[25] L. A. Anchordoqui, H. Goldberg, and G. Steigman, Right-handed neutrinos as the dark radiation: Status and forecasts for the LHC, Phys. Lett. B **718**, 1162 (2013).
[26] D. Buarque Franzosi, M. T. Frandsen, and I. M. Shoemaker, New or ν missing energy: Discriminating dark matter from neutrino interactions at the LHC, Phys. Rev. D **93**, 095001 (2016).
[27] S. Davidson and V. Sanz, Non-standard neutrino interactions at colliders, Phys. Rev. D **84**, 113011 (2011).
[28] S. Davidson and V. Sanz, Non standard neutrino interactions at LEP2 and the LHC, J. Phys. Conf. Ser. **408**, 012033 (2013).
[29] A. Friedland, M. L. Graesser, I. M. Shoemaker, and L. Vecchi, Probing nonstandard Standard Model backgrounds with LHC monojets, Phys. Lett. B **714**, 267 (2012).
[30] D. Choudhury, K. Ghosh, and S. Niyogi, Non-standard neutrino interactions: Obviating oscillation experiments, arXiv:1801.01513.
[31] J. Liao, D. Marfatia, and K. Whisnant, Degeneracies in long-baseline neutrino experiments from nonstandard interactions, Phys. Rev. D **93**, 093016 (2016).
[32] P. Coloma and T. Schwetz, Generalized mass ordering degeneracy in neutrino oscillation experiments, Phys. Rev. D **94**, 055005 (2016); Erratum **95**, 079903(E) (2017).
[33] K. N. Deepthi, S. Goswami, and N. Nath, Can nonstandard interactions jeopardize the hierarchy sensitivity of DUNE?, Phys. Rev. D **96**, 075023 (2017).

[34] K. N. Deepthi, S. Goswami, and N. Nath, Challenges posed by non-standard neutrino interactions in the determination of δ_{CP} at DUNE, arXiv:1711.04840.
[35] M. Masud, A. Chatterjee, and P. Mehta, Probing CP violation signal at DUNE in presence of non-standard neutrino interactions, J. Phys. G **43**, 095005 (2016).
[36] A. de Gouvêa and K. J. Kelly, Non-standard neutrino interactions at DUNE, Nucl. Phys. **B908**, 318 (2016).
[37] P. Coloma, Non-Standard Interactions in propagation at the Deep Underground Neutrino Experiment, J. High Energy Phys. 03 (2016) 016.
[38] C. Soumya and R. Mohanta, Implications of lepton flavor violation on long baseline neutrino oscillation experiments, Phys. Rev. D **94**, 053008 (2016).
[39] M. Blennow, S. Choubey, T. Ohlsson, D. Pramanik, and S. K. Raut, A combined study of source, detector and matter non-standard neutrino interactions at DUNE, J. High Energy Phys. 08 (2016) 090.
[40] D. V. Forero and P. Huber, Hints for Leptonic *CP* Violation or New Physics?, Phys. Rev. Lett. **117**, 031801 (2016).
[41] K. Huitu, T. J. Kärkkäinen, J. Maalampi, and S. Vihonen, Constraining the nonstandard interaction parameters in long baseline neutrino experiments, Phys. Rev. D **93**, 053016 (2016).
[42] M. Masud and P. Mehta, Nonstandard interactions spoiling the *CP* violation sensitivity at DUNE and other long baseline experiments, Phys. Rev. D **94**, 013014 (2016).
[43] M. Masud and P. Mehta, Nonstandard interactions and resolving the ordering of neutrino masses at DUNE and other long baseline experiments, Phys. Rev. D **94**, 053007 (2016).
[44] S. K. Agarwalla, S. S. Chatterjee, and A. Palazzo, Degeneracy between θ_{23} octant and neutrino non-standard interactions at DUNE, Phys. Lett. B **762**, 64 (2016).
[45] J. Liao, D. Marfatia, and K. Whisnant, Nonmaximal neutrino mixing at NOνA from nonstandard interactions, Phys. Lett. B **767**, 350 (2017).
[46] S. Fukasawa, M. Ghosh, and O. Yasuda, Is nonstandard interaction a solution to the three neutrino tensions?, arXiv:1609.04204.
[47] M. Blennow, P. Coloma, E. Fernandez-Martinez, J. Hernandez-Garcia, and J. Lopez-Pavon, Non-unitarity, sterile neutrinos, and non-standard neutrino interactions, J. High Energy Phys. 04 (2017) 153.
[48] J. Liao, D. Marfatia, and K. Whisnant, Nonstandard neutrino interactions at DUNE, T2HK and T2HKK, J. High Energy Phys. 01 (2017) 071.
[49] M. Ghosh and O. Yasuda, Effect of systematics in the T2HK, T2HKK, and DUNE experiments, Phys. Rev. D **96**, 013001 (2017).
[50] M. Ghosh and O. Yasuda, Testing NSI suggested by the solar neutrino tension in T2HKK and DUNE, arXiv:1709.08264.
[51] A. N. Khan, D. W. McKay, and F. Tahir, Sensitivity of medium-baseline reactor neutrino mass-hierarchy experiments to nonstandard interactions, Phys. Rev. D **88**, 113006 (2013).
[52] T. Ohlsson, H. Zhang, and S. Zhou, Nonstandard interaction effects on neutrino parameters at medium-baseline reactor antineutrino experiments, Phys. Lett. B **728**, 148 (2014).
[53] I. Girardi, D. Meloni, and S. T. Petcov, The Daya Bay and T2K results on $\sin^2 2\theta_{13}$ and non-standard neutrino interactions, Nucl. Phys. **B886**, 31 (2014).
[54] A. Di Iura, I. Girardi, and D. Meloni, Probing new physics scenarios in accelerator and reactor neutrino experiments, J. Phys. G **42**, 065003 (2015).
[55] S. K. Agarwalla, P. Bagchi, D. V. Forero, and M. Tórtola, Probing non-standard interactions at Daya Bay, J. High Energy Phys. 07 (2015) 060.
[56] M. Blennow, S. Choubey, T. Ohlsson, and S. K. Raut, Exploring source and detector non-standard neutrino interactions at ESSνSB, J. High Energy Phys. 09 (2015) 096.
[57] C. Patrignani *et al.* (Particle Data Group Collaboration), Review of particle physics, Chin. Phys. C **40**, 100001 (2016).
[58] M. Blennow, P. Coloma, and E. Fernandez-Martinez, Reassessing the sensitivity to leptonic CP violation, J. High Energy Phys. 03 (2015) 005.
[59] S. M. Davidson and H. E. Logan, Dirac neutrinos from a second Higgs doublet, Phys. Rev. D **80**, 095008 (2009).
[60] P. A. N. Machado, Y. F. Perez, O. Sumensari, Z. Tabrizi, and R. Z. Funchal, On the viability of minimal neutrinophilic two-Higgs-doublet models, J. High Energy Phys. 12 (2015) 160.
[61] V. Zarikas, The phase transition of the two Higgs extension of the standard model, Phys. Lett. B **384**, 180 (1996).
[62] A. B. Lahanas, V. C. Spanos, and V. Zarikas, Charge asymmetry in two-Higgs doublet model, Phys. Lett. B **472**, 119 (2000).
[63] G. Aliferis, G. Kofinas, and V. Zarikas, Efficient electroweak baryogenesis by black holes, Phys. Rev. D **91**, 045002 (2015).
[64] E. Ma, Naturally Small Seesaw Neutrino Mass with No New Physics Beyond the TeV Scale, Phys. Rev. Lett. **86**, 2502 (2001).
[65] S. Gabriel and S. Nandi, A new two Higgs doublet model, Phys. Lett. B **655**, 141 (2007).
[66] S. Knapen, T. Lin, and K. M. Zurek, Light dark matter: Models and constraints, Phys. Rev. D **96**, 115021 (2017).
[67] S. Sadhukhan and S. Mohanty, Explanation of IceCube spectrum with $\nu \to 3\nu$ neutrino splitting in a ν2HDM model, arXiv:1802.09498.
[68] G. Abbiendi *et al.* (LEP, DELPHI, OPAL, ALEPH, and L3 Collaboration), Search for charged Higgs bosons: Combined results using LEP data, Eur. Phys. J. C **73**, 2463 (2013).
[69] SLD Electroweak Group, SLD Heavy Flavor Group, DELPHI, LEP, ALEPH, OPAL, LEP Electroweak Working Group, L3 Collaboration, A combination of preliminary electroweak measurements and constraints on the standard model, arXiv:hep-ex/0312023.
[70] P. J. Fox, R. Harnik, J. Kopp, and Y. Tsai, LEP shines light on dark matter, Phys. Rev. D **84**, 014028 (2011).
[71] T. Fukuyama and K. Tsumura, Detecting Majorana nature of neutrinos in muon decay, arXiv:0809.5221.
[72] J. Adam *et al.* (MEG Collaboration), New Constraint on the Existence of the $\mu^+ \to e^+\gamma$ Decay, Phys. Rev. Lett. **110**, 201801 (2013).

[73] E. Bertuzzo, Y. F. Perez G., O. Sumensari, and R. Zukanovich Funchal, Limits on neutrinophilic two-Higgs-doublet models from flavor physics, J. High Energy Phys. 01 (2016) 018.
[74] K. Hayasaka *et al.*, Search for lepton flavor violating tau decays into three leptons with 719 million produced tau + tau-pairs, Phys. Lett. B **687**, 139 (2010).
[75] A. Dedes and H. E. Haber, Can the Higgs sector contribute significantly to the muon anomalous magnetic moment?, J. High Energy Phys. 05 (2001) 006.
[76] J. A. Grifols and R. Pascual, Contribution of charged Higgs bosons to the anomalous magnetic moment of the muon, Phys. Rev. D **21**, 2672 (1980).
[77] P. A. R. Ade *et al.* (Planck Collaboration), Planck 2015 results. XIII. Cosmological parameters, Astron. Astrophys. **594**, A13 (2016).
[78] K. A. Olive, G. Steigman, and T. P. Walker, Primordial nucleosynthesis: Theory and observations, Phys. Rep. **333**, 399 (2000).
[79] J. Zhang and S. Zhou, Relic right-handed Dirac neutrinos and implications for detection of cosmic neutrino background, Nucl. Phys. **B903**, 211 (2016).
[80] A. V. Berkov, Y. P. Nikitin, A. L. Sudarikov, and M. Y. Khlopov, Possible manifestations of an anomalous 4ν interaction, Yad. Fiz. **48**, 779 (1988).
[81] K. M. Belotsky, A. L. Sudarikov, and M. Y. Khlopov, Constraint on anomalous 4ν interaction, Yad. Fiz. **64**, 1718 (2001).
[82] K. M. Belotsky, A. L. Sudarikov, and M. Y. Khlopov, Constraints on triplet Majoron model due to observations of neutrinos from stellar collapse, Yad. Fiz. **47**, 891 (1988).
[83] C. Adams *et al.* (LBNE Collaboration), The long-baseline neutrino experiment: Exploring fundamental symmetries of the Universe, arXiv:1307.7335.
[84] R. Acciarri *et al.* (DUNE Collaboration), Long-Baseline Neutrino Facility (LBNF) and Deep Underground Neutrino Experiment (DUNE) Conceptual Design Report Volume 1: The LBNF and DUNE Projects, arXiv:1601.05471.
[85] J. Strait *et al.* (DUNE Collaboration), Long-Baseline Neutrino Facility (LBNF) and Deep Underground Neutrino Experiment (DUNE) Conceptual Design Report Volume 3: Long-Baseline Neutrino Facility for DUNE June, 2015, arXiv:1601.05823.
[86] R. Acciarri *et al.* (DUNE Collaboration), Long-Baseline Neutrino Facility (LBNF) and Deep Underground Neutrino Experiment (DUNE) Conceptual Design Report, Volume 4 The DUNE Detectors at LBNF, arXiv:1601.02984.
[87] R. Acciarri *et al.* (DUNE Collaboration), Long-Baseline Neutrino Facility (LBNF) and Deep Underground Neutrino Experiment (DUNE) Conceptual Design Report Volume 2: The Physics Program for DUNE at LBNF, arXiv:1512.06148.
[88] M. C. Gonzalez-Garcia and M. Maltoni, Atmospheric neutrino oscillations and new physics, Phys. Rev. D **70**, 033010 (2004).
[89] G. L. Fogli, E. Lisi, A. Marrone, D. Montanino, and A. Palazzo, Getting the most from the statistical analysis of solar neutrino oscillations, Phys. Rev. D **66**, 053010 (2002).
[90] R. Gandhi, P. Ghoshal, S. Goswami, P. Mehta, S. U. Sankar, and S. Shalgar, Mass hierarchy determination via future atmospheric neutrino detectors, Phys. Rev. D **76**, 073012 (2007).
[91] P. Huber, M. Lindner, and W. Winter, Simulation of long-baseline neutrino oscillation experiments with GLoBES (General Long Baseline Experiment Simulator), Comput. Phys. Commun. **167**, 195 (2005).
[92] P. Huber, J. Kopp, M. Lindner, M. Rolinec, and W. Winter, New features in the simulation of neutrino oscillation experiments with GLoBES 3.0: General Long Baseline Experiment Simulator, Comput. Phys. Commun. **177**, 432 (2007).
[93] M. D. Messier, Ph.D. thesis, Boston University, 1999.
[94] E. A. Paschos and J. Y. Yu, Neutrino interactions in oscillation experiments, Phys. Rev. D **65**, 033002 (2002).
[95] N. Nath, M. Ghosh, and S. Goswami, The physics of antineutrinos in DUNE and determination of octant and δ_{CP}, Nucl. Phys. **B913**, 381 (2016).
[96] P. F. de Salas, D. V. Forero, C. A. Ternes, M. Tortola, and J. W. F. Valle, Status of neutrino oscillations 2017, Phys. Lett. B **782**, 633 (2018).
[97] F. Capozzi, E. Lisi, A. Marrone, D. Montanino, and A. Palazzo, Neutrino masses and mixings: Status of known and unknown 3ν parameters, Nucl. Phys. **B908**, 218 (2016).
[98] M. C. Gonzalez-Garcia, M. Maltoni, and T. Schwetz, Global analyses of neutrino oscillation experiments, Nucl. Phys. **B908**, 199 (2016).